

Article

Easy Processing of Metal–Organic Frameworks into Pellets and Membranes

Flávio Figueira ^{1,*}, Ricardo F. Mendes ^{1,*}, Eddy M. Domingues ², Paula Barbosa ²,
Filipe Figueiredo ², Filipe A. A. Paz ^{1,*} and João Rocha ^{1,*}

¹ Department of Chemistry, CICECO—Aveiro Institute of Materials, Universidade de Aveiro, 3810-193 Aveiro, Portugal

² Department of Materials & Ceramic Engineering, CICECO—Aveiro Institute of Materials, University of Aveiro, 3810-193 Aveiro, Portugal; eddy@ua.pt (E.M.D.); paula.barbosa@ua.pt (P.B.); lebre@ua.pt (F.F.)

* Correspondence: ffigueira@ua.pt (F.F.); rfmendes@ua.pt (R.F.M.); filipe.paz@ua.pt (F.A.A.P.); rocha@ua.pt (J.R.); Tel.: +351-234-401-418 (F.F. & R.F.M. & F.A.A.P. & J.R.); Fax: +351-234-401-470 (F.F. & R.F.M. & F.A.A.P. & J.R.)

† The authors contributed equally to his work.

Received: 6 December 2019; Accepted: 16 January 2020; Published: 22 January 2020



Featured Application: The methods presented provide the know-how for the immobilization of metal–organic frameworks (MOFs) in the form of pellets and membranes with increased water repellency, known for its competitive ability for MOFs binding sites with air contaminants. These methods can provide advances in the preparation of filters for the removal of toxic compounds in air purification devices.

Abstract: Herein, we present a simple and inexpensive method for the immobilization of Metal–Organic Framework (MOF) particles in the form of pellets and membranes. This processing procedure is possible using polymethacrylate polymer (PMMA) as a binding or coating agent, improving stability and significantly increasing the water repellency. HKUST and M²MOF-74 (M = Mg²⁺, Zn²⁺, Co²⁺ or Ni²⁺) are stable with the processing and high loadings of MOF materials into the processed pellet or membranes. These methods can provide the know-how for the immobilization of MOFs for, for example, application in air purification and the removal of toxic compounds and are well-suited for deployment in air purification devices.

Keywords: metal–organic frameworks; processing; pellet; membrane

1. Introduction

Metal–Organic Frameworks (MOFs) are a versatile and broad class of crystalline materials with high porosity and a massive internal surface area [1–3]. These properties and the extraordinary diversity of their organic and inorganic building units make MOFs highly relevant in applications such as catalysis, sensors, batteries, biomedicine, and food safety [4–8]. Due to their synthetic versatility, long-range order, rich host–guest chemistry, uniform pore size, and high surface area, MOFs are particularly well-suited for the adsorption of a wide range of anthropogenic hazardous pollutants including NO_x, SO_x, CO, H₂S, NH₃, HCN, volatile organic compounds (VOCs), and polycyclic aromatic compounds (PAHs). Most of these pollutants are classified as toxic/carcinogenic and pose a global risk to the environment and human health. However, in order to successfully be used in these applications, MOFs must be both stable, featuring exceptional properties, and processed in a form that enables their integration into devices [9]. The use of processing methods that afford a certain degree of cohesion and allow shaping, and the spatial orientation of the crystals as needed, while interfacing

with other components of the device [10]. Indeed, the use of suitable processing methodologies determines the usefulness of a material, allowing it to perform at its best [11]. Notwithstanding, MOF integration into devices is still a challenging task because most synthesis takes place inside sealed glass tubes under solvothermal conditions, yielding very insoluble powders formed by randomly aggregated crystallites making it impossible to apply in most of the currently available technologies. In this context, much of the present research focuses on developing MOF processing methods [12]. Although some MOF materials have already been processed into textiles [13], membranes [14,15], non-woven fabrics [16], and nanofibers [17], most of the processing methods used are complex and difficult to transpose to industry. Here, we propose a simple and efficient method for processing MOFs into pellets, and to incorporate them into membrane supports. We target the application of these materials in filters in air purifiers. HKUST and MMOF-74 (where $M = \text{Mg}^{2+}$, Zn^{2+} , Co^{2+} , or Ni^{2+}) were synthesized and processed in the form of pellets and membranes. These MOFs were selected due to their well-known capability to adsorb harmful indoor gases, namely CO_2 , CO , and SO_2 [18–29]. MOF materials were prepared and characterized by X-ray diffraction and scanning electron microscopy. Because of the strong competition of water molecules with these harmful gases, water adsorption isotherms of materials in the powder, and pellet forms were measured. Pellets were prepared by a simple and cost-efficient extrusion method using only water as the “binding agent”. The stability of these pellets was evaluated in terms of temperature and humidity.

2. Materials and Methods

2.1. General Instrumentation

Scanning electron microscopy (SEM) images were collected on a high-resolution microscope equipped with a Schottky emission gun (Hitachi SU-70 (4 kV)) with a working distance of about 10 mm. Samples were prepared by deposition on aluminum sample holders followed by carbon coating performed on a carbon evaporator (Emitech K950).

Fourier transform infrared (FT-IR) spectra ($4000\text{--}400\text{ cm}^{-1}$) were recorded using KBr pellets (VWR BDH Prolabo, SpectrosoL, FT-IR grade; typically, 2 mg of sample were mixed in a mortar with 200 mg of KBr) on a Mattson 7000 galaxy series spectrometer equipped with a DTGS CsI detector, or on a Bruker Tensor 27 spectrometer by averaging 256 scans at a maximum resolution of 2 cm^{-1} .

Routine powder X-ray diffraction (PXRD) data were collected at ambient temperature on an X'Pert MPD Philips diffractometer ($\text{Cu K}\alpha_1$ X-radiation, $\lambda_1 = 1.540598\text{ \AA}$; $\lambda_2 = 1.544426\text{ \AA}$), equipped with an X'Celerator detector and a flat-plate sample holder in a Bragg–Brentano para-focusing optics configuration (45 kV, 40 mA). Intensity data were collected by the step-counting method (step 0.04°), in continuous mode, in the ca. $5 \leq 2\theta \leq 50^\circ$ range.

The water vapor sorption isotherms were measured on a dynamic vapor sorption apparatus from surface measurement systems, using N_2 as the carrier gas (Air Liquide Alphagaz, less than 3 ppm H_2O , the total flow of 200 sccm). Dry aliquots (ca. 20 mg) were loaded in a steel pan and suspended in the measuring chamber. The experiment started with a 2 h pre-treatment at $150\text{ }^\circ\text{C}$, to completely dry the sample, followed by the isotherm at $25\text{ }^\circ\text{C}$ with increasing and decreasing relative humidity (RH) steps from 0% to 98%. Each humidity step was kept until the rate of change of mass per fixed time (dm/dt) was lower than 0.002%, for at least 10 min.

2.2. Reagents

2,5-Dihydroxyterephthalic acid (97%); benzene-1,3,5-tricarboxylic acid (95%); $\text{Mg}(\text{NO}_3)_2 \cdot 6\text{H}_2\text{O}$ (99.8%), $\text{CoCl}_2 \cdot 6\text{H}_2\text{O}$ (99%), $\text{Zn}(\text{OAc})_2 \cdot 2\text{H}_2\text{O}$ (98%), and $\text{Ni}(\text{NO}_3)_2 \cdot 6\text{H}_2\text{O}$ (97%) were obtained from Sigma-Aldrich. Dimethylformamide and ethanol of analytical grade were obtained from Carlo Erba. KBr for infrared spectroscopy was obtained from BDH SpectrosoL. Methyl methacrylate polymer (PMMA) was obtained from TCI. All chemicals were used as received without further purification.

2.3. Synthesis

2.3.1. MOF-74 Family

The following procedures were reproduced from Liao et al. with minor modifications [30].

MgMOF-74: 2,5-Dihydroxyterephthalic acid (0.66 g, 3.39 mmol) and $\text{Mg}(\text{NO}_3)_2 \cdot 6\text{H}_2\text{O}$ (2.86 g, 11.1 mmol) were mixed and dispersed in DMF/EtOH/ H_2O (*v/v/v*, 15/1/1, 300 mL) in a PTFE lined autoclave (500 mL). After complete dissolution, the vial was capped tightly and placed in an oven at 125 °C. After 20 h, the vial was removed from the oven and allowed to cool to ambient temperature. The resulting yellow microcrystals were collected and washed with DMF. The solvent exchange with ethanol was performed 3 times a day for 2 days.

CoMOF-74: 2,5-Dihydroxyterephthalic acid (0.50 g, 2.52 mmol) and $\text{CoCl}_2 \cdot 6\text{H}_2\text{O}$ (2.01 g, 8.45 mmol) were mixed and dispersed in DMF/EtOH/ H_2O (*v/v/v*, 1:1:1, 200 mL) in a PTFE lined autoclave (500 mL). The vial was capped tightly and placed in an oven at 100 °C. After 24 h, the vial was removed from the oven and allowed to cool to ambient temperature. The microcrystals were collected and washed with DMF. The solvent in the sample was exchanged with ethanol 3 times a day for 2 days.

NiMOF-74: 2,5-Dihydroxyterephthalic acid (0.51 g, 2.52 mmol) and $\text{Ni}(\text{NO}_3)_2 \cdot 6\text{H}_2\text{O}$ (2.41 g, 8.32 mmol) were mixed and dispersed in DMF/EtOH/ H_2O (*v/v/v*, 1:1:1, 200 mL) in a PTFE lined autoclave (500 mL). After complete dissolution, the vial was capped tightly and placed in an oven at 100 °C. After 24 h, the vial was removed from the oven and allowed to cool to ambient temperature. The microcrystals were collected and washed with DMF. The solvent in the sample was exchanged with ethanol at least 3 times a day for 2 days.

ZnMOF-74: 2,5-Dihydroxyterephthalic acid (1.02 g, 5.04 mmol) and $\text{Zn}(\text{OAc})_2 \cdot 2\text{H}_2\text{O}$ (4.43 g, 20.1 mmol) were dissolved in 90 mL of DMF with stirring, followed by the addition of 5 mL of distilled water. The mixture was heated in an oven at 100 °C for 20 h. After decanting the supernatant, the product was rinsed with DMF and immersed in ethanol for 2 days, during which time the activation solvent was decanted and replaced three times.

2.3.2. HKUST

Benzene-1,3,5-tricarboxylic acid (2.10 g, 9.99 mmol) and $\text{Cu}(\text{acac})_2$ (4.03 g, 15.4 mmol) were mixed and dispersed in DMF/EtOH/ H_2O (*v/v/v*, 1/1/1, 100 mL) in a PTFE lined autoclave (150 mL). After complete dissolution, the vial was capped tightly and placed in an oven at 80 °C. After 20 h, the vial was removed from the oven and allowed to cool to ambient temperature. The resulting blue microcrystals were collected and washed with DMF.

2.4. Pellet Preparation

Pellets were prepared using a home-made extrusion apparatus with an external heating source. In summary, 500 μL of water was added dropwise to 500 mg of MOF until the formation of a malleable paste. Subsequently, this paste is introduced into an extrusion apparatus, and the final pellet is dried at ambient conditions.

2.5. Membrane Preparation

A suspension containing 50 mg of HKUST or MOF-74 in 10 mL CH_2Cl_2 was stirred for 15 min. To this suspension, 150 mg of polymethylmethacrylate (PMMA) in powder was added and left stirring for 30 min. The remaining viscous solution was then cast in a glass petri dish and left unstirred at ambient conditions until complete evaporation of the solvents.

3. Results and Discussion

3.1. MOF Synthesis

The synthesis of HKUST and a series of MMOF-74 (where M = Mg²⁺, Zn²⁺, Co²⁺, or Ni²⁺) was adapted from the work of Omar Farha's group [30], affording gram-scale amounts of the target materials. Scaling up of MOFs synthesis often leads to the formation of undesired phases. However, our materials are pure and present good crystallinity (Figure 1). Regarding the MOF-74 family, depending on the metal center used, different crystal sizes and morphologies are obtained (Figure 1, insert). MgMOF-74 and CoMOF-74 present large block-like crystals with sizes comprehended between 25 and 50 μm, while NiMOF-74 and ZnMOF-74 have reduced crystal sizes with a thin plate or spherical-like shape significantly smaller than the previous congeners (below 10 μm).

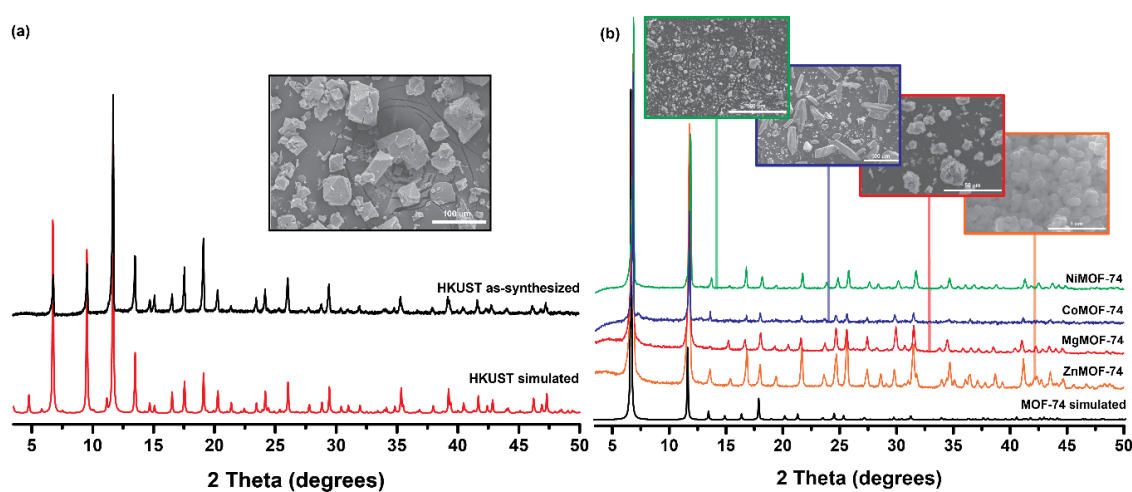


Figure 1. Powder X-ray diffractograms and SEM images of (a) HKUST and (b) MOF-74 family.

3.2. Water Adsorption Studies

One of the drawbacks of using MOFs in adsorption applications is the competition between the target gases and water molecules [31]. Many MOFs have high water uptakes [32]. For example, Yahgi's group reported an aluminum bearing MOF capable of adsorbing water from desert air with an incredible efficiency [33].

Water adsorption isotherms measured at 25 °C in order to ascertain the amount of water adsorbed at different relative humidity (RH, 20–98%) As expected, both HKUST and MgMOF-74 show an increase in water adsorption with increasing RH, reaching a total of 36.1% and 31.5% mass uptake at 98% RH since both materials exhibit large pores and surface areas (Figure 2 and Figure S1). In contrast, while ZnMOF-74 shows a similar water adsorption profile (with a total of 24.5%), Co- and NiMOF-74 present very small water uptakes (under 6%), even at high RH (98%). The metal center has a vital role in the water adsorption process. Moreover, it is observed a significant hysteresis behavior in the adsorption/desorption process of Mg- and ZnMOF-74 in comparison to Co- and NiMOF-74 (with the ratio between adsorption/desorption ca. two times higher for Mg- and ZnMOF-74).

Previous reports show a correlation between the hysteresis water vapor sorption and desorption isotherms curves with increasing cation radii [34]. However, this correlation is not observed here, since nickel and cobalt show a lower hysteresis than magnesium and yet have a larger size. In this case, the adsorption mechanism is not achieved mainly by interaction with the metallic nodes. As previously reported, water molecules can also interact with the material itself via hydrogen bonding, which ultimately can lead to a change in this trend. [35,36].

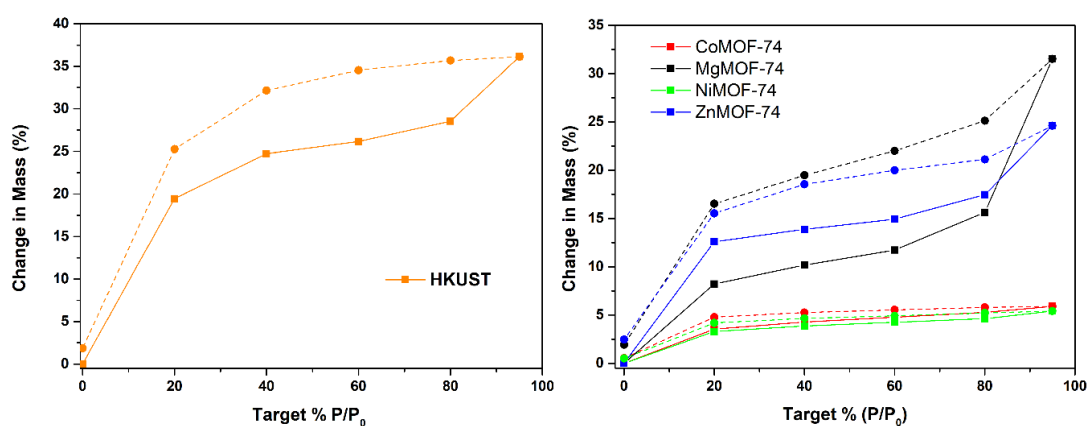


Figure 2. Water vapor sorption and desorption isotherms curves for HKUST and MOF-74 series at 25 °C. Straight lines and dashed lines represent the adsorption and desorption processes, respectively.

3.3. MOF Processing

3.3.1. Pellets

In this work, pellets of all materials were obtained by a simple extrusion method, whereby a small amount of water is added to the corresponding MOF powder. The resulting paste is then loaded into a syringe and heated, as depicted in Figure 3a. The processing of these materials into pellets were chosen due to two main reasons: it is a simple and inexpensive processing method, which can be advantageous to transpose to industry; and, in terms of engineering in industrial practice MOFs, are required to be pelletized and packed into columns for real gas capture and process studies [37].

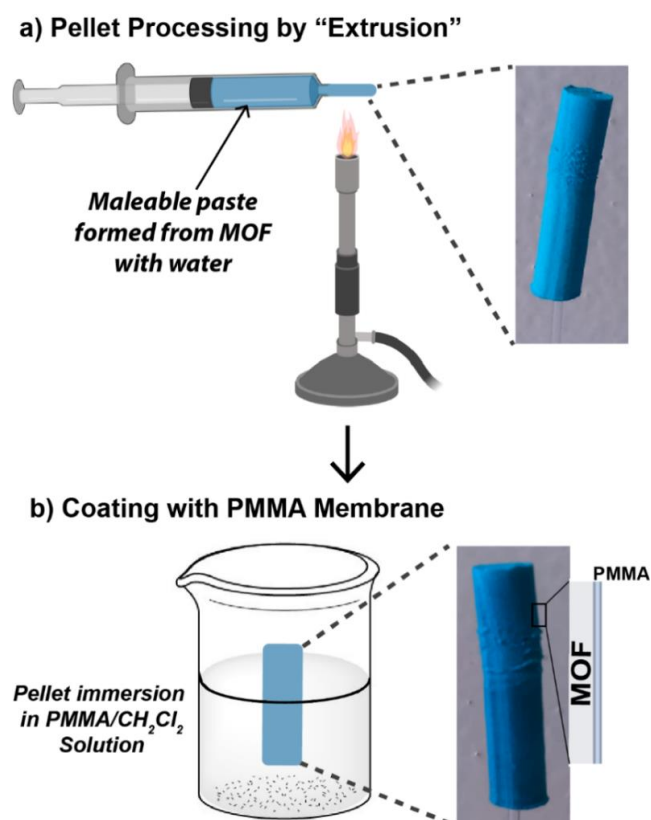


Figure 3. Schematic representation of (a) pellet preparation process by an extrusion method and (b) pellet coating with polymethacrylate polymer (PMMA).

Depending on the form of extrusion used, the materials can be processed into different sizes and shapes (Figure 4), and in large quantities, effortlessly. The pellets were characterized by powder X-ray diffraction, showing that this process preserves the structural integrity of the materials (Figure S2).

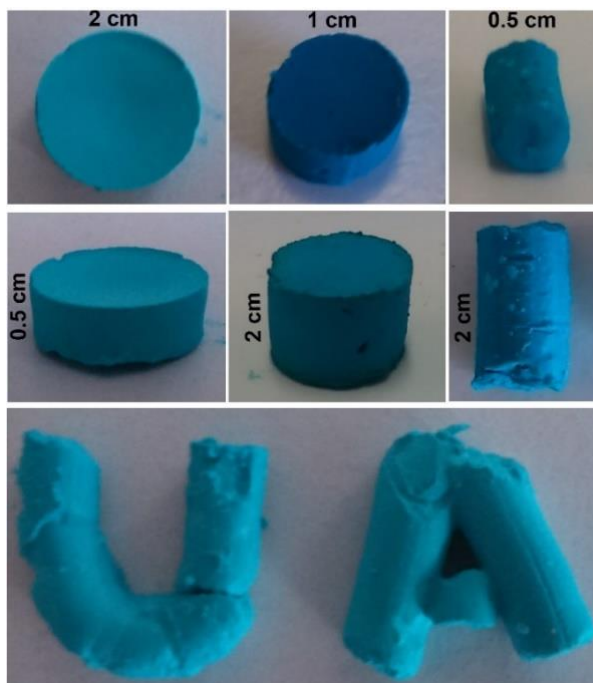


Figure 4. HKUST processed into pellets with different sizes and in the UA (University of Aveiro) words.

Despite the rapid and straightforward pellet preparation method, with time, the lack of binding agent causes the pellets to peel off, presumably due to their dehydration. To circumvent this problem, we used a coating with methyl methacrylate polymer (PMMA), which has already found application in membranes for CO₂ removal in submarines [38]. PMMA coating enables the MOF adsorption of target gas molecules while preventing contact with water molecules. The coating process is straightforward, as depicted in Figure 3b. The pellets are immersed in a PMMA solution in dichloromethane and left to dry at ambient conditions and preserve their integrity for months.

Subsequently, we assessed the water stability of uncoated and PMMA coated pellets. As shown in Figure 5, the uncoated pellets immediately disaggregate after immersion. In contrast, the coated pellets preserve their integrity even after one week immersed in distilled water.

Pellets were then introduced for 72 h in a desiccator containing a saturated solution of magnesium nitrate or potassium sulfate to simulate exposure to ca. 54% and 98% RH, respectively. At 54% RH, the coated pellets maintain their integrity, while the uncoated pellets already show some degradation (not shown). At 98% RH, the uncoated HKUST and MgMOF-74 pellets were cracked or even completely disaggregated, while the coated pellets bearing showed no visible degradation (Figure 6).

Interestingly, the integrity of the CoMOF-74 pellet remains the same at high RH even without PMMA coating. This behavior is attributed to the low water adsorption of Co- and NiMOF-74 (Section 3.2). All coated materials maintain their structural integrity in 98% RH (Figure 7).

To better understand the (un)coated pellets' behavior in humid conditions, water vapor isotherms were also measured at 25 °C for HKUST. As shown in Figure 8, the processing into pellets decreases considerably the water adsorption of HKUST (ca. 10% water uptake at 98% RH). This response can be explained by the reduced contact surface of crystals when compared to the powder form. Interestingly, the coated and uncoated pellets show approximately the same water uptake and similar isotherms. Thus, the coating process only maintains the pellet form and does not change the water uptake.

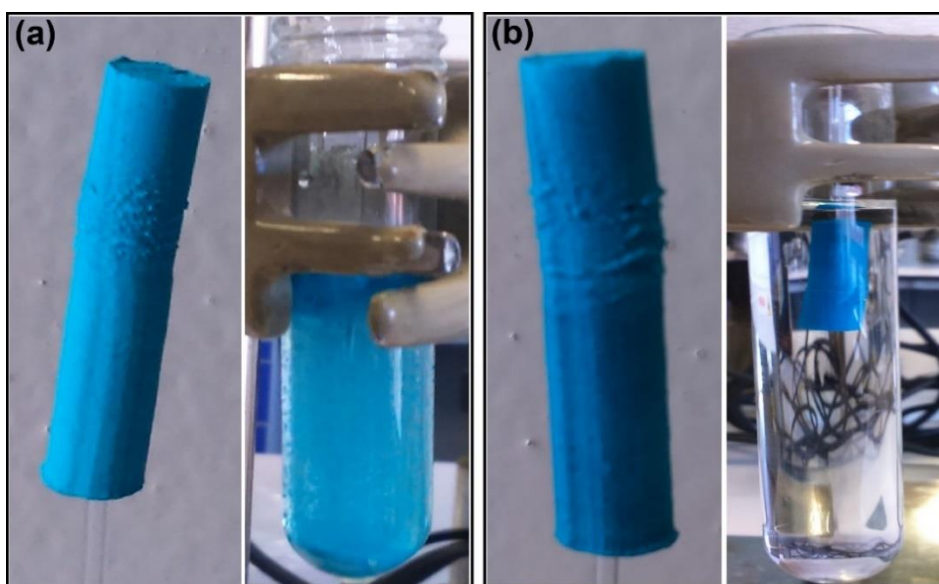
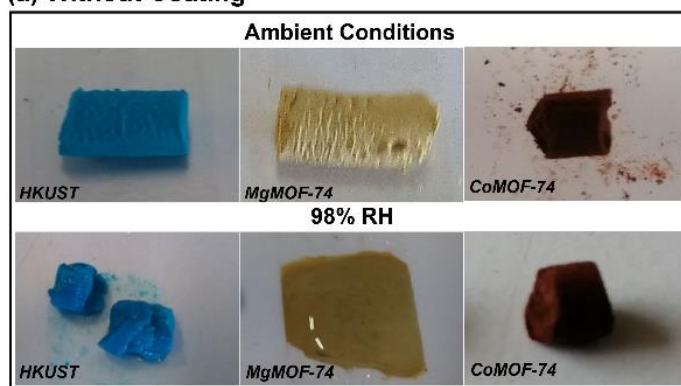


Figure 5. HKUST-1 pellets (a) uncoated and (b) PMMA coated, before and after water immersion (for a period of three weeks).

(a) Without Coating



(b) With PMMA Coating

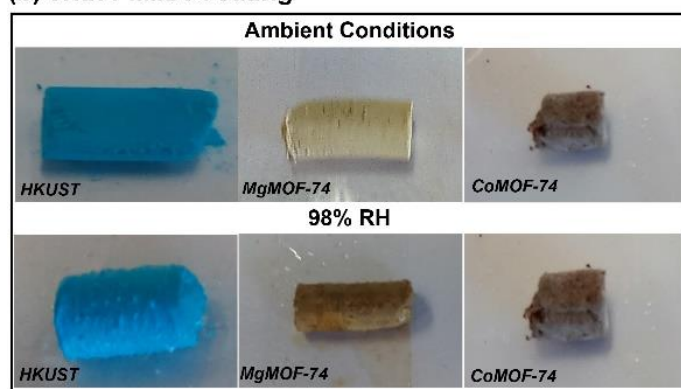


Figure 6. (a) Uncoated and (b) PMMA coated metal–organic frameworks (MOF) pellets under laboratory conditions, and after 72 h in a chamber with 98% relative humidity (RH).

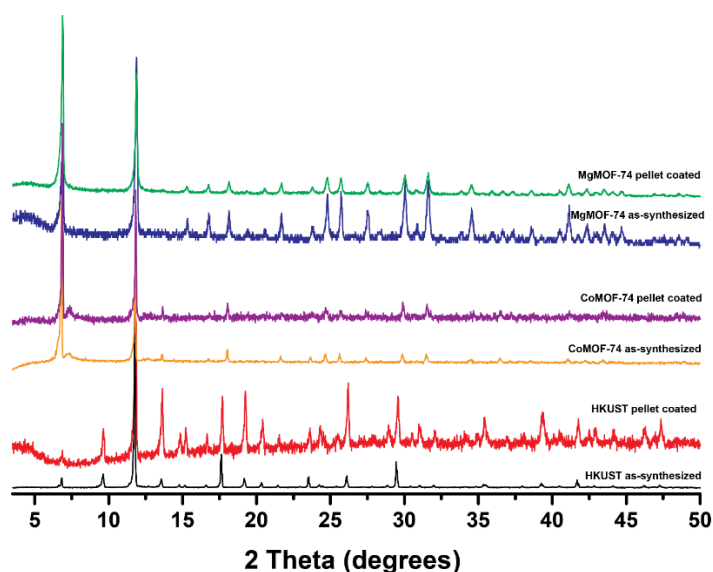


Figure 7. Powder X-ray diffractograms of MgMOF-74, CoMOF-74, and HKUST pellets coated with PMMA after three days at 98% RH.

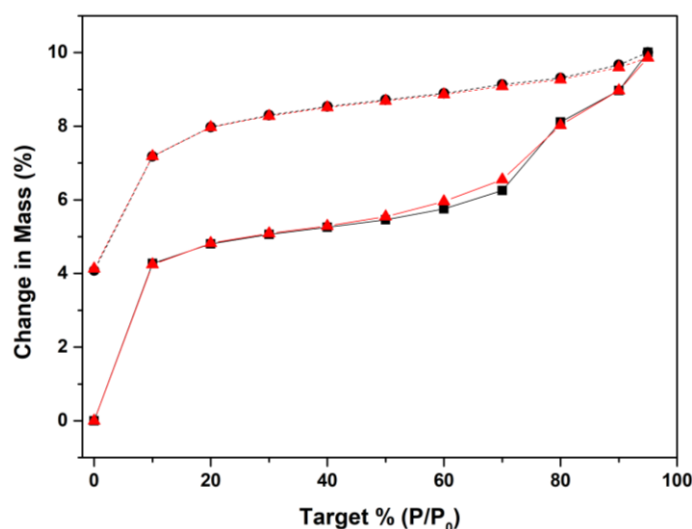


Figure 8. Water vapor sorption and desorption isotherms curves for coated (red) and uncoated (black) HKUST pellets measured at 25 °C. Straight and dashed lines represent the adsorption and desorption processes, respectively.

Gas molecules trapped inside MOF pores may be easily removed, increasing the temperature. For this reason, the stability of the prepared pellets was accessed under different temperature conditions. Here, we only illustrate these studies with HKUST pellets.

Pellets were submitted to different cycles of increase–decrease temperature. After coating, pellets were introduced in an oven, heated at 125 °C for 24 h, and allowed to cool down to ambient temperature (this process was repeated four times). Most MOFs used as gas sorbents are regenerated at a temperature of 125 °C. The structural integrity of the pellets after each cycle was analyzed by powder X-ray diffraction. As observed in Figure 9, the material preserves its structure and crystallinity, even after four cycles. No visible change is observed in the pellets except for some small black areas, probably associated with the PMMA film pointing that the PMMA coating can increase the overall pellet stability significantly.

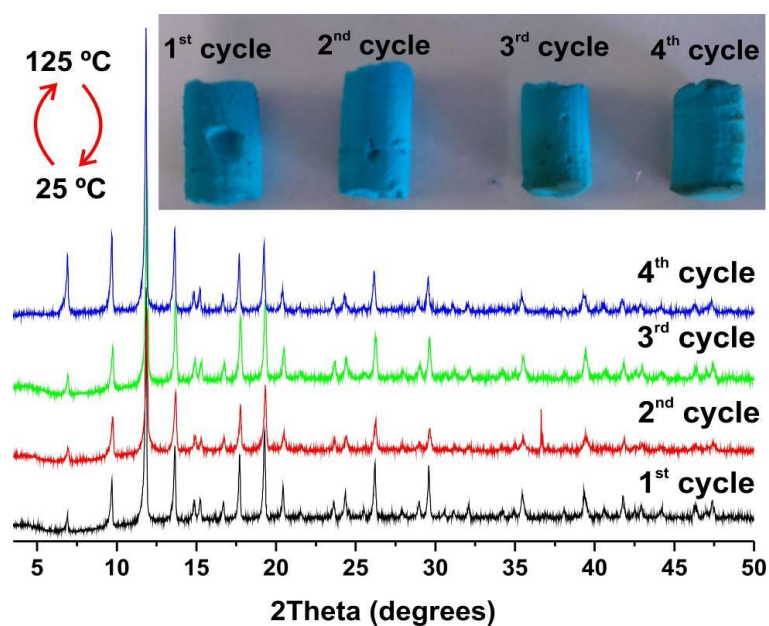


Figure 9. Powder X-ray diffraction of HKUST pellets after different cycles of increase–decrease of temperature; (inset) images of the pellets after each cycle of thermal treatment.

3.3.2. Membranes

MOFs materials were processed into filters using the PMMA as the support. MOFs in the powder form were suspended in a PMMA solution in dichloromethane and cast into a mold. After solvent evaporation, an MOF@PMMA membrane was obtained (MOFs preserving their structure and crystallinity, Figure S3).

As observed in Figures 10 and 11, HKUST and Mg-MOF-74 are homogeneously distributed over the entire membrane. Membranes with a higher amount of MOF material can also be obtained, but they are fragile and brittle. A MOF:PMMA mass ratio of 1:3 is the highest possible without compromising the membrane elasticity. Humidity and temperature tests of these membranes were carried out. Due to the insolubility of PMMA in water, membranes show no change at high RH. On the other hand, at temperatures above 140 °C, membranes become fragile and break.

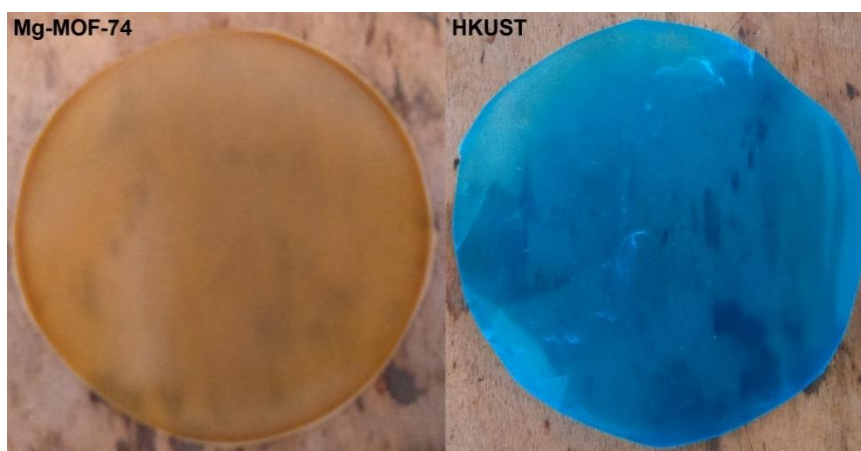


Figure 10. MgMOF-74 and HKUST supported in a PMMA membrane.

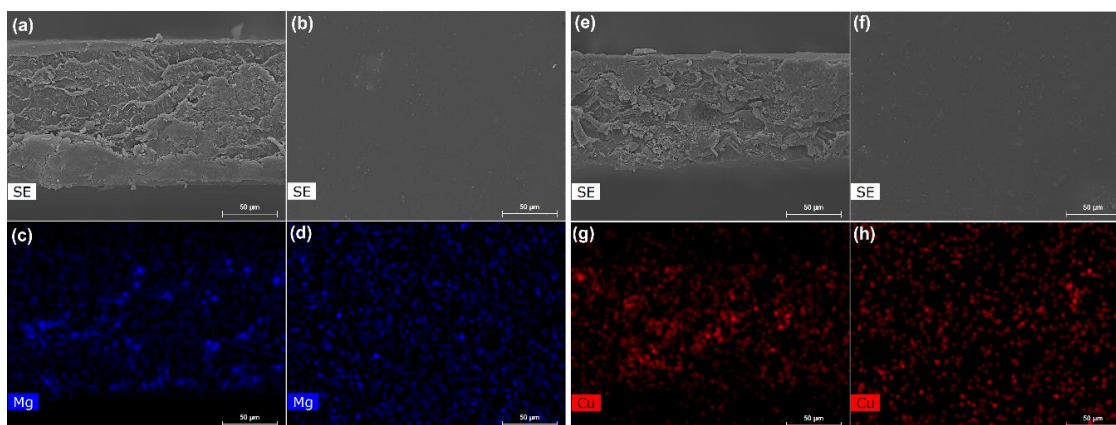


Figure 11. SEM images of (a) cross-section, (b) surface (c,d), and corresponding EDS magnesium elemental mapping of MgMOF-74@PMMA membrane; (e) cross-section and (f) surface (g,h), and corresponding EDS copper elemental mapping on HKUST@PMMA membrane.

4. Conclusions

In summary, we present a versatile and straightforward approach to the integration of MOF into pellets and membranes. The processing of HKUST-1 and MMOF-74 ($M = \text{Mg}^{2+}$, Zn^{2+} , Co^{2+} , or Ni^{2+}) in pellets and membranes achieved high MOF loadings. Pellet processing was carried out by a simple extrusion method using water as the “binding agent”. Furthermore, the studied materials were also supported into PMMA membranes with a simple procedure where the materials stay homogeneously distributed over the entire membrane. These are stable up 140 °C and high RH.

Over time, the MOFs pellets peel off, and their stability is improved with polymethacrylate polymer coating: no deterioration was observed at 98% RH and 125 °C. Likewise, the MOF membranes also proved stable in high humidity conditions, without loss of structural integrity and crystallinity.

Supplementary Materials: The following are available online at <https://www.mdpi.com/2076-3417/10/3/798/s1>, Figure S1—Structures of HKUST and MOF-74 MOFs emphasizing the open metal sites present; Figure S2—Powder X-ray diffractograms of the studied materials, as-synthesized and after processing into pellets; Figure S3—Powder X-ray diffractograms of (a) HKUST and (b) MgMOF-74 after incorporation in a PMMA membrane.

Author Contributions: The work here presented was developed in a highly collaborative environment where, F.F. and R.F.M. performed the MOF synthesis, pellet/membrane preparation, characterization, and overall writing of the paper. E.M.D. and P.B. performed water adsorption studies in powder and pellet form. F.F., F.A.A.P. and J.R. foresaw and supervised the general guidelines of the work, as well as the writing of the paper. All authors have read and agreed to the published version of the manuscript.

Funding: This work was developed within the scope of the project CICECO-Aveiro Institute of Materials, UIDB/50011/2020 & UIDP/50011/2020, financed by national funds through the FCT/MEC and when appropriate co-financed by FEDER under the PT2020 Partnership Agreement and UniRCell (SAICTPAC/0032/2015, POCI-01-0145-FEDER-016422. F.F. and R.F.M. acknowledge the project “Smart Green Homes—BOSCH” (POCI-010247-FEDER-007678) for the Postdoctoral and Masters scholarships (refs. BPD/CICECO/5508/2017 and BIM-SGH/CICECO-UA/174-01/2017, respectively). FCT is also gratefully acknowledged for the Junior Research Position CEECIND/00553/2017 (to R.F.M.)

Conflicts of Interest: The authors declare no conflicts of interest.

References

- Zhou, H.-C.; Long, J.R.; Yaghi, O.M. Introduction to Metal–Organic Frameworks. *Chem. Rev.* **2012**, *112*, 673–674. [[CrossRef](#)]
- Van Vleet, M.J.; Weng, T.; Li, X.; Schmidt, J.R. In Situ, Time-Resolved, and Mechanistic Studies of Metal–Organic Framework Nucleation and Growth. *Chem. Rev.* **2018**, *118*, 3681–3721. [[CrossRef](#)] [[PubMed](#)]
- Das, S.; Heasman, P.; Ben, T.; Qiu, S. Porous Organic Materials: Strategic Design and Structure–Function Correlation. *Chem. Rev.* **2017**, *117*, 1515–1563. [[CrossRef](#)] [[PubMed](#)]

4. Wang, P.-L.; Xie, L.-H.; Joseph, E.A.; Li, J.-R.; Su, X.-O.; Zhou, H.-C. Metal–Organic Frameworks for Food Safety. *Chem. Rev.* **2019**, *119*, 10638–10690. [[CrossRef](#)] [[PubMed](#)]
5. Rice, A.M.; Martin, C.R.; Galitskiy, V.A.; Berseneva, A.A.; Leith, G.A.; Shustova, N.B. Photophysics Modulation in Photoswitchable Metal–Organic Frameworks. *Chem. Rev.* **2019**. [[CrossRef](#)]
6. Wang, Q.; Astruc, D. State of the Art and Prospects in Metal–Organic Framework (MOF)-Based and MOF-Derived Nanocatalysis. *Chem. Rev.* **2019**. [[CrossRef](#)]
7. Zhu, L.; Liu, X.-Q.; Jiang, H.-L.; Sun, L.-B. Metal–Organic Frameworks for Heterogeneous Basic Catalysis. *Chem. Rev.* **2017**, *117*, 8129–8176. [[CrossRef](#)]
8. Maurin, G.; Serre, C.; Cooper, A.; Férey, G. The new age of MOFs and of their porous-related solids. *Chem. Soc. Rev.* **2017**, *46*, 3104–3107. [[CrossRef](#)]
9. Abid, H.R.; Ang, H.M.; Wang, S.B. Effects of ammonium hydroxide on the structure and gas adsorption of nanosized Zr-MOFs (UiO-66). *Nanoscale* **2012**, *4*, 3089–3094. [[CrossRef](#)]
10. Burtch, N.C.; Heinen, J.; Bennett, T.D.; Dubbeldam, D.; Allendorf, M.D. Mechanical Properties in Metal–Organic Frameworks: Emerging Opportunities and Challenges for Device Functionality and Technological Applications. *Adv. Mater.* **2018**, *30*, 1704124. [[CrossRef](#)]
11. Falcaro, P.; Ricco, R.; Doherty, C.M.; Liang, K.; Hill, A.J.; Styles, M.J. MOF positioning technology and device fabrication. *Chem. Soc. Rev.* **2014**, *43*, 5513–5560. [[CrossRef](#)] [[PubMed](#)]
12. Rodríguez-San-Miguel, D.; Zamora, F. Processing of covalent organic frameworks: An ingredient for a material to succeed. *Chem. Soc. Rev.* **2019**, *48*, 4375–4386. [[CrossRef](#)] [[PubMed](#)]
13. Zhang, K.; Huo, Q.; Zhou, Y.-Y.; Wang, H.-H.; Li, G.-P.; Wang, Y.-W.; Wang, Y.-Y. Textiles/Metal–Organic Frameworks Composites as Flexible Air Filters for Efficient Particulate Matter Removal. *ACS Appl. Mater. Interfaces* **2019**, *11*, 17368–17374. [[CrossRef](#)] [[PubMed](#)]
14. Liang, H.; Jiao, X.; Li, C.; Chen, D. Flexible self-supported metal–organic framework mats with exceptionally high porosity for enhanced separation and catalysis. *J. Mater. Chem. A* **2018**, *6*, 334–341. [[CrossRef](#)]
15. Adatoz, E.; Avci, A.K.; Keskin, S. Opportunities and challenges of MOF-based membranes in gas separations. *Sep. Purif. Technol.* **2015**, *152*, 207–237. [[CrossRef](#)]
16. Li, P.; Li, J.; Feng, X.; Li, J.; Hao, Y.; Zhang, J.; Wang, H.; Yin, A.; Zhou, J.; Ma, X.; et al. Metal-organic frameworks with photocatalytic bactericidal activity for integrated air cleaning. *Nat. Commun.* **2019**, *10*, 2177. [[CrossRef](#)]
17. Bian, Y.; Wang, R.; Wang, S.; Yao, C.; Ren, W.; Chen, C.; Zhang, L. Metal–organic framework-based nanofiber filters for effective indoor air quality control. *J. Mater. Chem. A* **2018**, *6*, 15807–15814. [[CrossRef](#)]
18. Chowdhury, P.; Bikkina, C.; Meister, D.; Dreisbach, F.; Gumma, S. Comparison of adsorption isotherms on Cu-BTC metal organic frameworks synthesized from different routes. *Microporous Mesoporous Mat.* **2009**, *117*, 406–413. [[CrossRef](#)]
19. Liang, Z.J.; Marshall, M.; Chaffee, A.L. Comparison of Cu-BTC and zeolite 13X for adsorbent based CO₂ separation. In *Greenhouse Gas Control Technologies 9*; Gale, J., Herzog, H., Braitsch, J., Eds.; Elsevier Science Bv: Amsterdam, The Netherlands, 2009; Volume 1, pp. 1265–1271.
20. Yazaydin, A.O.; Benin, A.I.; Faheem, S.A.; Jakubczak, P.; Low, J.J.; Willis, R.R.; Snurr, R.Q. Enhanced CO₂ Adsorption in Metal-Organic Frameworks via Occupation of Open-Metal Sites by Coordinated Water Molecules. *Chem. Mat.* **2009**, *21*, 1425–1430. [[CrossRef](#)]
21. Hamon, L.; Jolimaitre, E.; Pirngruber, G.D. CO₂ and CH₄ Separation by Adsorption Using Cu-BTC Metal-Organic Framework. *Ind. Eng. Chem. Res.* **2010**, *49*, 7497–7503. [[CrossRef](#)]
22. Millward, A.R.; Yaghi, O.M. Metal-organic frameworks with exceptionally high capacity for storage of carbon dioxide at room temperature. *J. Am. Chem. Soc.* **2005**, *127*, 17998–17999. [[CrossRef](#)] [[PubMed](#)]
23. Aprea, P.; Caputo, D.; Gargiulo, N.; Iucolano, F.; Pepe, F. Modeling Carbon Dioxide Adsorption on Microporous Substrates: Comparison between Cu-BTC Metal-Organic Framework and 13X Zeolitic Molecular Sieve. *J. Chem. Eng. Data* **2010**, *55*, 3655–3661. [[CrossRef](#)]
24. Mason, J.A.; Sumida, K.; Herm, Z.R.; Krishna, R.; Long, J.R. Evaluating metal-organic frameworks for post-combustion carbon dioxide capture via temperature swing adsorption. *Energy Environ. Sci.* **2011**, *4*, 3030–3040. [[CrossRef](#)]
25. Bao, Z.B.; Yu, L.A.; Ren, Q.L.; Lu, X.Y.; Deng, S.G. Adsorption of CO₂ and CH₄ on a magnesium-based metal organic framework. *J. Colloid Interface Sci.* **2011**, *353*, 549–556. [[CrossRef](#)]

26. Farrusseng, D.; Daniel, C.; Gaudillere, C.; Ravon, U.; Schuurman, Y.; Mirodatos, C.; Dubbeldam, D.; Frost, H.; Snurr, R.Q. Heats of Adsorption for Seven Gases in Three Metal-Organic Frameworks: Systematic Comparison of Experiment and Simulation. *Langmuir* **2009**, *25*, 7383–7388. [[CrossRef](#)]
27. Britt, D.; Tranchemontagne, D.; Yaghi, O.M. Metal-organic frameworks with high capacity and selectivity for harmful gases. *Proc. Natl. Acad. Sci. USA* **2008**, *105*, 11623–11627. [[CrossRef](#)]
28. Liu, J.; Wang, Y.; Benin, A.I.; Jakubczak, P.; Willis, R.R.; LeVan, M.D. CO₂/H₂O Adsorption Equilibrium and Rates on Metal-Organic Frameworks: HKUST-1 and Ni/DOBDC. *Langmuir* **2010**, *26*, 14301–14307. [[CrossRef](#)]
29. Llewellyn, P.L.; Bourrelly, S.; Serre, C.; Vimont, A.; Daturi, M.; Hamon, L.; De Weireld, G.; Chang, J.S.; Hong, D.Y.; Hwang, Y.K.; et al. High uptakes of CO₂ and CH₄ in mesoporous metal-organic frameworks MIL-100 and MIL-101. *Langmuir* **2008**, *24*, 7245–7250. [[CrossRef](#)]
30. Liao, Y.J.; Zhang, L.; Weston, M.H.; Morris, W.; Hupp, J.T.; Farha, O.K. Tuning ethylene gas adsorption via metal node modulation: Cu-MOF-74 for a high ethylene deliverable capacity. *Chem. Commun.* **2017**, *53*, 9376–9379. [[CrossRef](#)]
31. Moliner, M.; Martinez, C.; Corma, A. Multipore Zeolites: Synthesis and Catalytic Applications. *Angew. Chem.-Int. Ed.* **2015**, *54*, 3560–3579. [[CrossRef](#)]
32. Canivet, J.; Fateeva, A.; Guo, Y.; Coasne, B.; Farrusseng, D. Water adsorption in MOFs: Fundamentals and applications. *Chem. Soc. Rev.* **2014**, *43*, 5594–5617. [[CrossRef](#)] [[PubMed](#)]
33. Fathieh, F.; Kalmutzki, M.J.; Kapustin, E.A.; Waller, P.J.; Yang, J.J.; Yaghi, O.M. Practical water production from desert air. *Sci. Adv.* **2018**, *4*. [[CrossRef](#)] [[PubMed](#)]
34. Wiśniewski, M.; Bieniek, A.; Bolibok, P.; Koter, S.; Bryk, P.; Kowalczyk, P.; Terzyk, A.P. Mechanistic aspects of water adsorption-desorption in porphyrin containing MOFs. *Microporous Mesoporous Mat.* **2019**, *290*, 109649. [[CrossRef](#)]
35. Tan, K.; Zuluaga, S.; Gong, Q.; Canepa, P.; Wang, H.; Li, J.; Chabal, Y.J.; Thonhauser, T. Water Reaction Mechanism in Metal Organic Frameworks with Coordinatively Unsaturated Metal Ions: MOF-74. *Chem. Mat.* **2014**, *26*, 6886–6895. [[CrossRef](#)]
36. Furukawa, H.; Gándara, F.; Zhang, Y.-B.; Jiang, J.; Queen, W.L.; Hudson, M.R.; Yaghi, O.M. Water Adsorption in Porous Metal–Organic Frameworks and Related Materials. *J. Am. Chem. Soc.* **2014**, *136*, 4369–4381. [[CrossRef](#)] [[PubMed](#)]
37. Hu, Z.; Wang, Y.; Shah, B.B.; Zhao, D. CO₂ Capture in Metal–Organic Framework Adsorbents: An Engineering Perspective. *Adv. Sustain. Syst.* **2019**, *3*, 1800080. [[CrossRef](#)]
38. Ali, U.; Karim, K.J.B.A.; Buang, N.A. A Review of the Properties and Applications of Poly (Methyl Methacrylate) (PMMA). *Polym. Rev.* **2015**, *55*, 678–705. [[CrossRef](#)]



© 2020 by the authors. Licensee MDPI, Basel, Switzerland. This article is an open access article distributed under the terms and conditions of the Creative Commons Attribution (CC BY) license (<http://creativecommons.org/licenses/by/4.0/>).